ARTHRITIS & RHEUMATISM
Vol. 65, No. 11, November 2013, pp 2814–2825
DOI 10.1002/art.38095

Role of ADAM-17, p38 MAPK, Cathepsins, and the Proteasome Pathway in the Synthesis and Shedding of Fractalkine/CX_3CL1 in Rheumatoid Arthritis

Brian A. Jones, Sharayah Riegsecker, Ayesha Rahman, Maria Beamer, Wissam Aboualaiwi, Sadik A. Khuder, and Salahuddin Ahmed

Objective. **To evaluate the mechanism of fractalkine (FKN)/CX_3CL1 synthesis and shedding in rheumatoid arthritis synovial fibroblasts (RASFs) and in rat adjuvant-induced arthritis (AIA).**

Methods. **The effect of tumor necrosis factor α (TNFα) and/or interferon-γ (IFNγ) on FKN synthesis and shedding in human RASFs was determined over time by immunostaining, quantitative reverse transcription–polymerase chain reaction, and Western blotting. The role of protease enzymes and signaling pathways was evaluated using chemical inhibitors and small interfering RNA (siRNA). The activity of 20S proteasome in the lysates and the DNA binding of NF-κB/p65 in the nuclear fractions were evaluated. The in vivo relevance of these findings was examined in rat AIA.**

Results. **In RASFs, stimulation with the combination of TNFα and IFNγ induced cellular expression of FKN within 24 hours. Activation of ADAM-17, but not ADAM-10, partly mediated the proteolytic shedding and release of soluble FKN (sFKN) following TNFα/IFNγ stimulation for 24–72 hours. Compared with control siRNA, ADAM-17 siRNA markedly inhibited TNFα/IFNγ-induced sFKN production (by ~33%). TNFα/IFNγ-induced sFKN release was markedly suppressed by inhibitors of ADAM-17, p38 MAPK, proteasome, or cathepsin inhibitor but not by inhibitors of caspase 3 or calpain. TNFα/IFNγ-induced proteasome activity also correlated with rapid degradation of IκBα and p38 MAPK phosphorylation. In vivo findings showed increased FKN expression in the joints of rats with AIA, which correlated with increased expression of ADAM-17 and phospho–p38 MAPK.**

Conclusion. **Our results provide new understanding of the role of ADAM-17, p38 MAPK, cathepsins, and the proteasome pathway in FKN expression and shedding. Regulating these pathways may suppress FKN-mediated inflammation and tissue destruction.**

Rheumatoid arthritis (RA) is a chronic inflammatory joint disease in which chemokines play an important role through the recruitment and retention of monocytes and T lymphocytes into joints, leading to hyperplasia of the synovial lining and the destruction of cartilage and bone (1–4). When synovial fibroblasts (SFs) are activated in response to inflammatory cytokines such as interleukin-1β (IL-1β), tumor necrosis factor α (TNFα), or interferon-γ (IFNγ), they release chemokines that can use their receptors to facilitate the accumulation of inflammatory cells at the site of inflammation (2). Chemokines are categorized into 4 subfamilies (C, CC, CXC, and CX3C) according to the number and spacing of the first 2 cysteines in a conserved cysteine (C) structural motif (5).

Recent studies have defined the pathologic significance of fractalkine (FKN)/CX_3CL1 in RA and other chronic diseases (6–11). Interestingly, FKN performs a dual function in an inflammatory situation based on its form. Soluble FKN (sFKN) consists of the chemokine domain and the extracellular mucin-like stalk and functions as a chemoattractant, while the membrane-bound

Supported in part by the NIH (grants AT-003633 and AR-055741 to Dr. Ahmed) and the University of Toledo (start-up funding to Dr. Ahmed).

Brian A. Jones, BS, Sharayah Riegsecker, MS, Ayesha Rahman, PhD, Maria Beamer, BS, Wissam Aboualaiwi, PhD, Sadik A. Khuder, PhD, Salahuddin Ahmed, PhD: University of Toledo, Toledo, Ohio.

Mr. Jones and Ms Riegsecker contributed equally to this work.

Address correspondence to Salahuddin Ahmed, PhD, University of Toledo, Department of Pharmacology, College of Pharmacy, Health Science Campus, MS 1015, 3000 Arlington Avenue, Toledo, OH 43614. E-mail: Salah.Ahmed@utoledo.edu.

Submitted for publication May 29, 2012; accepted in revised form July 11, 2013.

form (referred to as FKN) functions as an adhesion molecule for CX_3CR1-expressing leukocytes. Soluble FKN is generated by the limited proteolysis of the disintegrin and metalloproteinases, ADAM-10 and ADAM-17/TNFα-converting enzyme (TACE), and functions as a chemoattractant (12–14). Besides its expression in macrophages, fibroblasts, endothelial cells, and dendritic cells in RA synovial tissue and synovial fluid, FKN is also expressed by RASFs and is released as sFKN during inflammation (15,16).

Recent studies suggest that TNFα significantly increases FKN expression in human umbilical vein endothelial cells (HUVECs) and rat aortic endothelial cells through the NF-κB signaling pathway (17,18). Treatment of HUVECs with a combination of IFNγ and TNFα synergistically induces FKN expression (19). In RASFs, synergistic induction with TNFα and IFNγ enhances FKN expression to a markedly greater level than induction with each cytokine alone (16). Despite the emerging role of FKN in RA pathogenesis, there has been limited success in achieving the development of therapies targeting FKN to ameliorate RA (20,21). This may be attributable to the limited understanding, particularly in terms of RA, of the molecular mechanisms governing FKN synthesis and enzymatic shedding in RASFs. A similar gap remains in our understanding of the role of specific ADAMs in mediating FKN processing in preclinical models of RA. The current study was carried out to decipher the steps involved in the molecular mechanism of FKN synthesis and shedding in RA pathogenesis, so that highly targeted therapeutic strategies targeting FKN may be developed.

MATERIALS AND METHODS

Antibodies and reagents. TNFα and IFNγ as well as goat anti-human FKN and anti-goat IgG horseradish peroxidase–linked secondary antibodies were purchased from R&D Systems. Inhibitors for the signaling pathways, caspase 3 (Z-DEVK-FMK), cathepsin (cathepsin inhibitor I), and calpain (calpeptin) were purchased from EMD Biosciences. The transfection reagents and small interfering RNA (siRNA) (control, ADAM-10, and ADAM-17) were purchased from Invitrogen Life Technologies. Human and rat FKN enzyme-linked immunosorbent assay (ELISA) kits were purchased from R&D Systems. Rabbit anti-human ADAM-17 and anti-human ADAM-10 antibodies were purchased from EMD Biosciences. Rabbit anti-human phosphorylation state–specific antibodies against JNK/SAPK, ERK-1/2, IκBα, and p38 MAPK were purchased from Cell Signaling Technology. MG-132 was purchased from Cayman Chemical. GM6001, an inhibitor of ADAM-17 and matrix metalloproteinases (MMPs), was purchased from Enzo Life Sciences. Actinomycin D, cycloheximide, and rabbit anti–β-actin antibody were purchased from Sigma-Aldrich.

Culture of human RASFs. Fibroblasts were isolated from the synovium of patients with RA, according to the University of Toledo Institutional Review Board–approved protocol, in compliance with the Declaration of Helsinki. These patients had undergone total joint replacement surgery or synovectomy and fulfilled the American College of Rheumatology 1987 revised criteria for the classification of RA (22). Fresh synovial tissue specimens were minced and digested in a solution of Dispase, collagenase, and DNase. Cells were used at passage 5–9, at which time they were a homogeneous population. RASFs were grown in RPMI 1640 medium with 10% fetal bovine serum (FBS) at 37°C in a humidified atmosphere with 5% CO_2. When confluent, the cells were passed by brief trypsinization. All treatments were performed in serum-free medium.

Treatment of RASFs. To evaluate the time-dependent effects of TNFα and/or IFNγ stimulation on FKN synthesis and shedding, RASFs (2×10^5/well) were plated in 6-well, flat-bottomed tissue culture plates (Corning) and cultured in RPMI 1640 plus 10% FBS until >80% confluent. RASFs were serum-starved overnight and the next day were stimulated with TNFα (20 ng/ml), IFNγ (10 ng/ml), or a combination of these cytokines for 24–72 hours. At the end of incubation, the conditioned medium was collected, and the cells were lysed in cell lysis buffer. These cells were used to study the time-dependent expression of FKN and its release as sFKN in the conditioned medium, by ELISA and Western blotting.

To study the signaling mechanism of FKN production induced by TNFα/IFNγ, RASFs were incubated with inhibitors of protein kinase C (PKC) (Ro-31; 10 μM), proteasome activity (MG132; 10 μM), p38 MAPK (SB203580; 10 μM), JNK/SAPK (SP600125; 10 μM), ERK-1/2 (PD98059; 10 μM), STAT-3 (AG-490; 10 μM), cathepsin (cathepsin I; 10 μM), and calpain (calpeptin; 100 nM) for 2 hours, followed by stimulation with TNFα/IFNγ for 72 hours. After 72 hours, the culture supernatant was collected and centrifuged at 10,000g for 5 minutes at 4°C to remove any particulate matter and stored at −80°C in fresh tubes. The production of sFKN was quantified in the collected supernatants, using commercially available ELISA kits (R&D Systems).

To study the effect of ADAM-17 and caspase 3 enzymes in mediating TNFα/IFNγ-induced FKN synthesis and shedding, RASFs were pretreated with ADAM-17 and MMP inhibitor (GM6001; 20 μM) and caspase 3 inhibitor (Z-DEVK-FMK; 10 μM) for 2 hours, followed by stimulation with TNFα/IFNγ for 24 hours and 72 hours. The expression of FKN was determined in the cell lysates obtained from the 24-hour treatment, whereas conditioned medium from the 72-hour treatment was concentrated and used for Western blot analysis.

Rat adjuvant-induced arthritis (AIA). Female Lewis rats weighing ~100 gm (Harlan) were injected subcutaneously at the base of the tail with 300 μl (5 mg/ml) of lyophilized *Mycobacterium butyricum* (Difco) in sterile mineral oil. The day of adjuvant injection was considered day 0. Ankle circumferences were measured on day 17 in a blinded manner, as described previously (23). The study also included a naive (no adjuvant) group for comparison. The ankle circumferences of both hind ankles from each rat were averaged, and n is the number of rats used in each experimental group. All animal studies were approved by the ethics committee of the University of Toledo.

Western blot analysis. To study the effects of TNFα (20 ng/ml) and/or IFNγ (10 ng/ml), cells were lysed in cell lysis buffer containing protease inhibitors (24,25). Protein was measured using a Pierce BCA Protein Assay Kit. Equal amounts of protein (20 μg) were loaded and separated by sodium dodecyl sulfate (SDS)–polyacrylamide gel electrophoresis and transferred onto nitrocellulose membranes (Bio-Rad). Blots were probed using rabbit polyclonal antibodies specific for FKN, ADAM-17, ADAM-10, and other signaling proteins. The immunoreactive protein bands were visualized using an enhanced chemiluminescence technique and were captured on developing film. Blots were stripped and reprobed with β-actin to ensure equal loading of the protein.

To study the possible effect of GM6001 on TNFα/IFNγ-induced MMP expression, we determined the level of extracellular matrix proteins MMP-1, MMP-2, MMP-3, MMP-8, MMP-9, and MMP-13, and tissue inhibitor of metalloproteinases 1 (TIMP-1), TIMP-2, TIMP-3, and TIMP-4 in the culture supernatants obtained from RASFs, using a human MMP antibody array (catalog no. AAH-MMP-1; RayBiotech) according to the manufacturer's protocol.

The ankles of rats in the AIA study were removed, snap-frozen, and homogenized on ice using a motorized homogenizer, followed by 30 seconds of sonication in 3 ml of phosphate buffered saline (PBS) containing Complete Protease Inhibitor Cocktail Minitablets (Roche). Homogenates were centrifuged at 2,500*g* for 10 minutes, filtered through a 0.45-μm pore–size filter (Millipore), and stored at −80°C until used. Protein concentrations were measured using a BCA Protein Assay Kit (Pierce). Western immunoblotting was performed to analyze joint homogenates (30 μg) for the expression of ADAM-17, ADAM-10, and phospho–p38 MAPK. The expression of proteins was normalized to the expression of their respective β-actins. Densitometric analysis of the relative expression of each protein was performed as previously described (23,26).

Gelatin zymography. MMP-2 activity in conditioned medium was measured as described previously (23,24). Briefly, 15 μl of conditioned medium was resolved under nonreducing conditions on SDS-polyacrylamide gels loaded with gelatin (1 mg/ml; type A from porcine skin) (Sigma) as a substrate. Following electrophoresis, the gels were washed with 2.5% Triton X-100 for 30 minutes followed by overnight incubation in developing buffer (50 m*M* Tris HCl, pH 8.0, 5 m*M* $CaCl_2$, and 0.02% NaN_3) at 37°C. Finally, gels were stained in Coomassie blue (R-250) and destained using 7% acetic acid and 5% methanol solution. Images of the digested regions representing MMP activity were captured and analyzed using ImageJ software (National Institutes of Health).

Transfection studies. To validate the role of ADAM-10 and ADAM-17 in FKN shedding, we performed transfection studies using commercially available siRNA for ADAM-10 and ADAM-17 and scrambled siRNA control (Life Technologies). RASFs were maintained in RPMI 1640 with 10% FBS and plated in 6-well plates to grow to ~50–60% confluence. Cells were transfected with 50 pmoles control, ADAM-10 siRNA, or ADAM-17 siRNA, using siRNA transfection reagent in serum-free RPMI 1640 without antibiotics, and left for 6 hours. Medium containing 20% FBS was then added, and the cells were grown for another 48 hours. After 48 hours, the cells were serum-starved overnight and then stimulated with TNFα/IFNγ for 72 hours. Conditioned medium was collected and processed as described above, for the detection of sFKN by ELISA. A pilot experiment was performed using 25, 50, and 75 pmoles siRNA prior to these experiments that showed optimum silencing of specific genes at 50 pmoles. Using a green fluorescent protein vector (a gift from Dr. Douglas Leaman, University of Toledo), we determined the siRNA transfection efficiency in RASFs, which was ~70–80% in RASFs, based on the quantitative analysis (data not shown).

Immunostaining. To verify the TNFα/IFNγ-induced time-dependent synthesis and shedding of FKN in RASFs, we performed immunostaining on these cells using a polyclonal antibody against FKN (R&D Systems). RASFs (1×10^4/well) in 8-well Lab-Tek chamber slides (BD Falcon) were left untreated or were treated with TNFα and IFNγ for 2, 6, 24, and 72 hours in serum-free RPMI 1640. Upon termination, the cells were washed with PBS and fixed with 4% paraformaldehyde containing 2% sucrose for 10 minutes, and then permeabilized with 1% Triton X-100 in PBS for 5 minutes. Slides were probed with goat polyclonal anti-FKN antibody (1 μg/ml) for 1 hour at room temperature in PBS, followed by PBS washes and incubation with biotinylated donkey anti-goat (10 μg/ml) antibody for 1 hour at room temperature. Texas Red-X/phalloidin (Invitrogen) that stains F-actin was used at a dilution of 1:500. Cover slides were then mounted with Vectashield mounting medium containing DAPI to counterstain DNA. For immunofluorescence studies, images (100× magnification) were captured under a Nikon TE2000 microscope equipped with a CoolSNAP EZ Monochrome Cooled CCD digital camera and analyzed using MetaMorph software (Molecular Devices).

RNA extraction and quantitative reverse transcription–polymerase chain reaction (qRT-PCR). Total RNA was isolated from human RASFs using RNAeasy Mini RNA isolation kits in conjunction with QIAshredders (Qiagen), according to the manufacturer's protocol. Following isolation, RNA was quantified and checked for purity using a spectrophotometer (NanoDrop Technologies). Complementary DNA was then prepared using a first-strand synthesis kit with anchored oligo(dT) RNA primers (Qiagen), according to the manufacturer's protocol.

Quantitative RT-PCR was performed using Platinum SYBR Green qPCR Master Mix (Qiagen) and specific primer sequences for human ADAM-17 (NM_003183), ADAM-10 (NM_001110), and β-actin (NM_001101) (Qiagen), using previously described methods (22,25). All samples were run in duplicate and analyzed using Eppendorf software (provided with the instrument). For quantification, the relative abundance of each gene was normalized to β-actin.

Assay of 20S proteasome activity. The proteasome activity in RASFs treated with TNFα and/or IFNγ was determined using a 20S proteasome activity assay kit according to the instructions provided by the manufacturer (Cayman Chemicals).

Preparation of nuclear extracts and NF-κB/p65 DNA-binding ELISA. To study proteasomal degradation of IκBα and subsequent activation of NF-κB mediating FKN synthesis and shedding, confluent RASFs were treated with TNFα (20 ng/ml) or IFNγ (10 ng/ml), alone and in combination, for 30 minutes in serum-free RPMI 1640. Upon termination, cells were washed with ice-cold PBS, collected by scraping, and centrifuged at 1,500*g* for 5 minutes at 4°C. Nuclear and cytoplasmic fractions from different treatment groups were

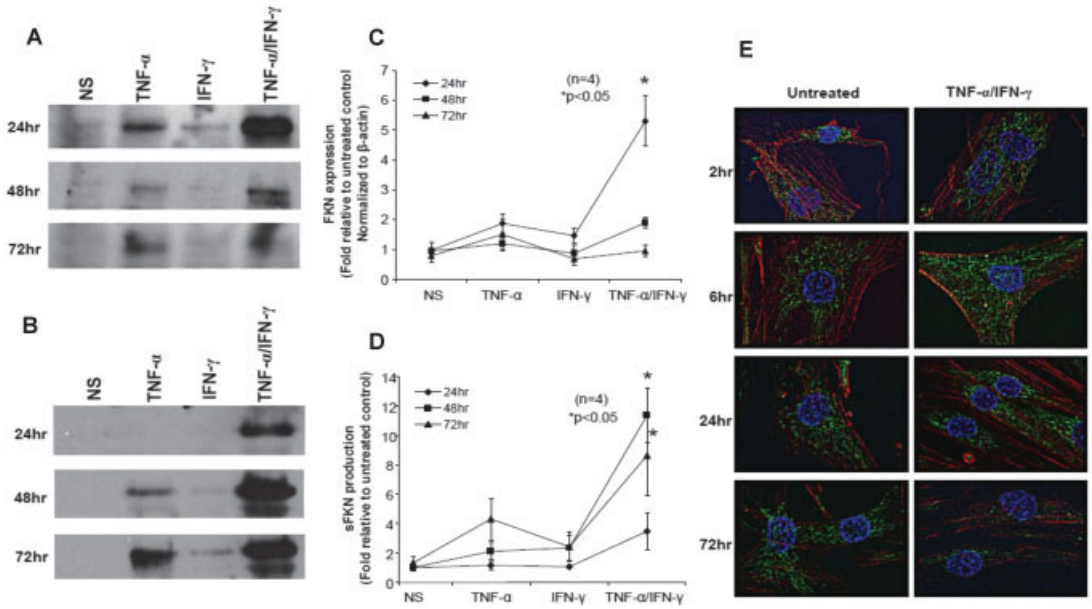

Figure 1. Time-dependent modulation of tumor necrosis factor α (TNFα)– and/or interferon-γ (IFNγ)–induced fractalkine (FKN) expression and soluble FKN (sFKN) release in rheumatoid arthritis synovial fibroblasts (RASFs). RASFs (2×10^5/well) were incubated in serum-free RPMI for 24, 48, or 72 hours, alone or with TNFα (20 ng/ml) and/or IFNγ (10 ng/ml). **A–D,** Expression and densitometric analysis of cellular FKN (**A** and **C**) and soluble FKN (**B** and **D**). The intensity of the bands was quantified using ImageJ software. Values are the mean ± SEM. **E,** FKN expression in untreated RASFs or RASFs treated with TNFα and/or IFNγ. Cells were immunostained with anti-FKN antibody (green), F-actin (red), and DAPI (blue). NS = not stimulated.

prepared as previously described (23,24). An equal amount of protein (15 μg) from nuclear and cytoplasmic fractions was evaluated for NF-κB/p65 expression by Western blotting. The nuclear extracts (5 μg) from 30 minutes of stimulation with TNFα and/or IFNγ were used to determine NF-κB/p65 DNA binding activity using commercially available DNA-binding ELISA kits (Active Motif).

Statistical analysis. Statistical analysis was performed using a Kruskal-Wallis nonparametric test followed by a Mann-Whitney U test to evaluate the statistical significance of group differences in measured parameters from sFKN ELISAs and protein expression studies in RASFs. Student's *t*-test was performed to calculate statistical differences between the means of the different protein variables obtained from in vivo findings. Due to the large variability in the protein expression profile from the joint homogenates in the rat AIA study (see Figures 6C and D), log transformation was performed to stabilize the values and satisfy the normality assumption of the parametric test. *P* values (2-tailed) less than 0.05 were considered significant.

RESULTS

Time-dependent synthesis and shedding of FKN in RASFs. To assess time-dependent synthesis and processing of FKN, we treated RASFs with TNFα/IFNγ for 24–72 hours. Stimulation with TNFα alone resulted in an almost 2-fold increase in FKN expression in RASFs (Figures 1A and C). IFNγ alone had no inducing effect but significantly potentiated the cellular expression of FKN induced by TNFα, to 5.3-fold within 24 hours, as compared with the untreated samples ($P < 0.05$) (Figures 1A and C). However, the level of cellular FKN expression decreased after 24 hours of TNFα/IFNγ stimulation (Figure 1C).

To confirm that the loss of FKN expression was attributable to its release, we concentrated culture supernatants and used them in Western blotting experiments to examine its release as sFKN. The results showed that only the combination of TNFα and IFNγ significantly enhanced the production of sFKN in RASFs within 24 hours and lasted up to 72 hours ($P < 0.05$) (Figures 1B and D). Densitometric analysis of the bands showed that TNFα/IFNγ stimulation caused 3.5-, 11.5-, and 9-fold increases in sFKN production at 24, 48, and 72 hours, respectively, when compared with untreated controls ($P < 0.05$, not stimulated versus 48 hours and 72 hours) (Figure 1D). In addition, TNFα alone induced an increase of ~4.5-fold in sFKN production by 72 hours when compared with the untreated controls ($P < 0.05$) (Figure 1D). Further validation of this observation by immunostaining analysis revealed

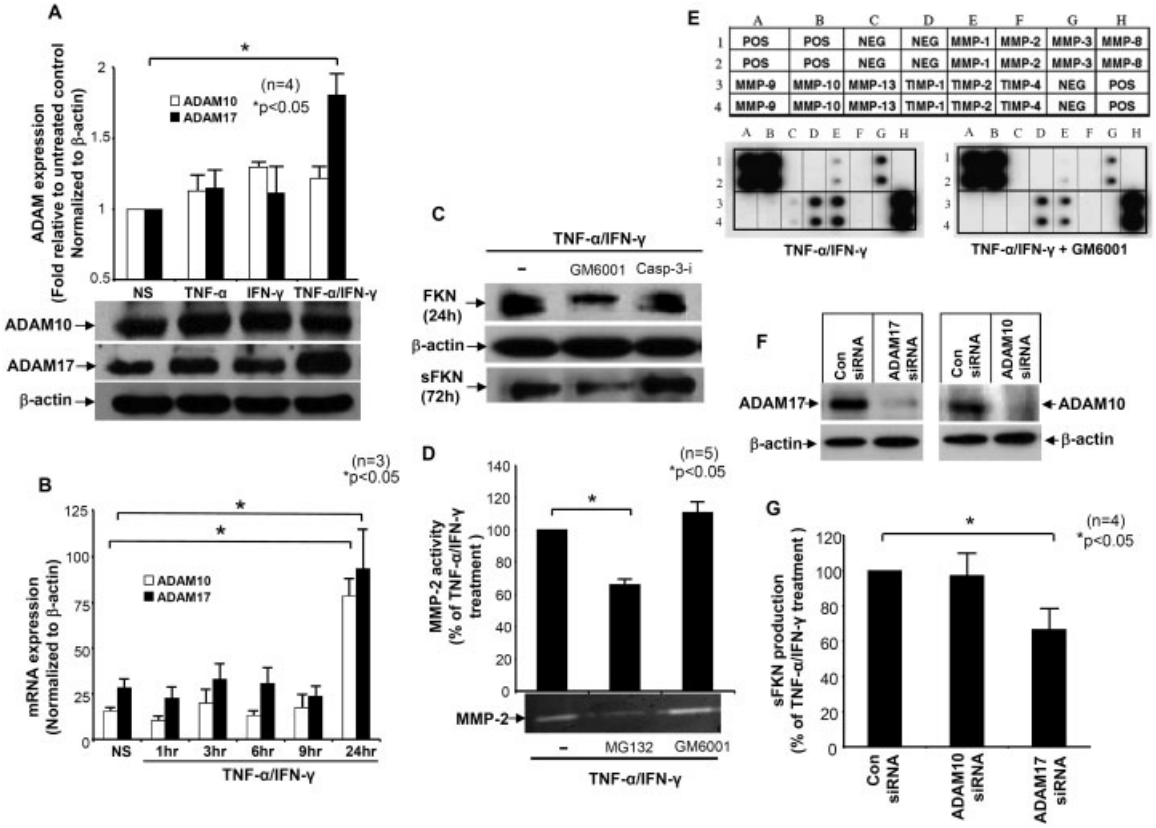

Figure 2. Partial involvement of TNFα/IFNγ-induced ADAM-17 in the expression and shedding of FKN in RASFs. **A,** ADAM-10 and ADAM-17 expression in RASFs (2×10^5/well) treated with TNFα and/or IFNγ for 24 hours, as determined by Western blotting. **B,** Messenger RNA expression in RASFs treated with TNFα and/or IFNγ for 24 hours, as determined by quantitative reverse transcription–polymerase chain reaction. **C,** FKN and sFKN expression in RASFs pretreated with GM6001 (20 μM) or the caspase 3 inhibitor (Casp-3-i) Z-DEV-FMK (10 μM) for 2 hours followed by TNFα/IFNγ stimulation for 24 and 72 hours, as determined by Western blotting. The blots shown are representative of 3 independent experiments using samples obtained from different donors. **D,** Matrix metalloproteinase 2 (MMP-2) activity in conditioned medium collected following treatment of RASFs with TNFα/IFNγ, with or without MG132 or GM6001, as determined by gelatin zymography. **E,** MMP/tissue inhibitor of metalloproteinases (TIMP) production in conditioned medium collected following treatment of SFs with TNFα/IFNγ with or without MG132 or GM6001 (pooled for each group), as determined using a human MMP antibody array kit according to the manufacturer's instructions. **F,** Efficiency of 50 pmoles ADAM-17 or ADAM-10 small interfering RNA (siRNA) in suppressing protein expression (n = 4). **G,** Soluble FKN levels in conditioned medium collected following transfection of RASFs with scrambled (Con), ADAM-10, or ADAM-17 siRNA followed by TNFα/IFNγ stimulation for 72 hours. Bars in **A, B, D,** and **G** are the mean ± SEM. See Figure 1 for other definitions.

that cellular FKN expression was increased within 6 hours of TNFα/IFNγ stimulation and peaked at ~24 hours (Figure 1E).

Involvement of ADAM-17, but not ADAM-10 or caspase 3, in TNFα/IFNγ-induced FKN shedding. Several studies suggest that FKN is processed as a soluble form by ADAM-17 under pathologic conditions, whereas ADAM-10 regulates the constitutive processing of FKN (13). For a clearer understanding of this mechanism, we determined the expression of ADAM-10 and ADAM-17 in RASFs. At the protein level, TNFα/IFNγ stimulation had no effect on ADAM-10, whereas ADAM-17 expression in RASFs increased by ~80% ($P < 0.05$) (Figure 2A). At the transcription level, TNFα/IFNγ stimulation increased messenger RNA (mRNA) expression of both ADAM-10 and ADAM-17 ~5-fold; however, only ADAM-17 protein expression was significantly increased in RASFs ($P < 0.05$) (Figure 2B).

To verify the role of ADAM-17 and other proteases such as caspase 3 in mediating TNFα/IFNγ-induced sFKN synthesis, we preincubated RASFs with inhibitors of ADAM-17/MMPs (GM6001) or caspase 3 (Z-DEVD-FMK) followed by TNFα/IFNγ stimulation. The results showed that caspase 3 inhibitor had no effect, whereas GM6001 partially blocked the synthesis and shedding of sFKN in RASFs (Figure 2C), suggesting the involvement of other signaling pathways in this

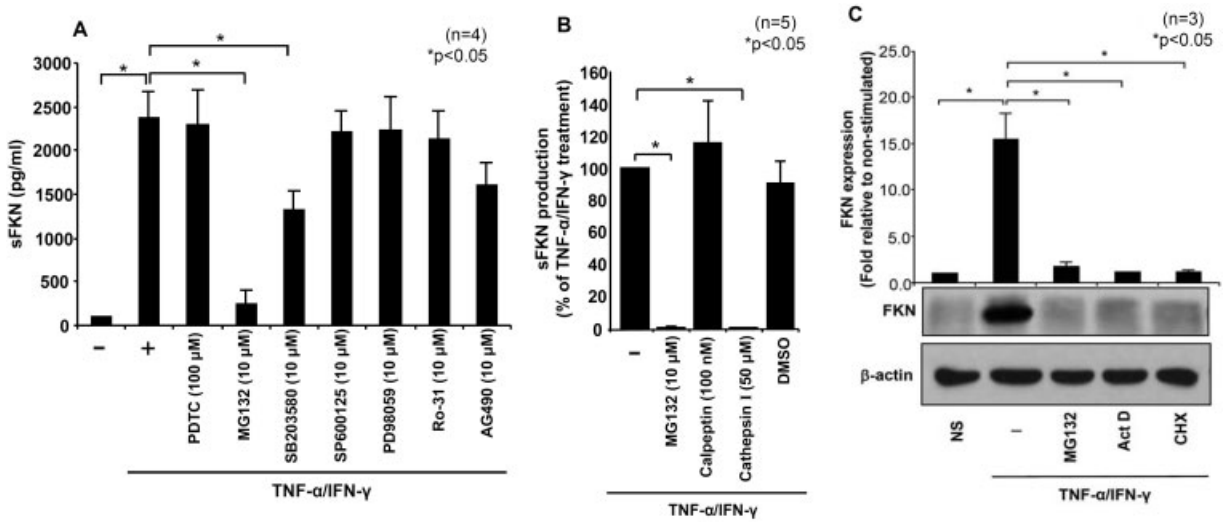

Figure 3. Involvement of the proteasome and p38 MAPK pathways in regulation of TNFα/IFNγ-induced sFKN production in RASFs. **A,** Production of sFKN in conditioned medium collected following preincubation of RASFs with inhibitors of proteasome activity (MG132), p38 MAPK (SB203580), JNK/SAPK (SP600125), ERK-1/2 (PD98059), protein kinase C (Ro-31), and STAT-3 (AG490) for 2 hours, followed by stimulation with TNFα/IFNγ for 72 hours, as determined by enzyme-linked immunosorbent assay (ELISA). **B,** Soluble FKN release in conditioned medium collected following pretreatment of RASFs with MG132, calpeptin, cathepsin inhibitor, or DMSO for 2 hours, followed by TNFα/IFNγ stimulation for 72 hours, as determined by ELISA. **C,** FKN expression in RASFs (2×10^5/well) pretreated with MG132, actinomycin D (Act D), and cycloheximide (CHX) for 1 hour, followed by TNFα/IFNγ stimulation for 24 hours. Cells were lysed in lysis buffer, and 20 μg of lysate from each sample was used to determine FKN expression. Bars show the mean ± SEM. PDTC = pyrrolidine dithiocarbamate (see Figure 1 for other definitions).

process. To verify that the inhibition of sFKN by GM6001 is due to the selective inhibition of ADAM-17, and possibly not other MMPs, we determined the catalytic activity of MMP-2, which is a major enzyme involved in joint destruction in RA (22,23). The results of zymography showed that MG132 significantly inhibited TNFα/IFNγ-induced MMP-2 activity in RASFs ($P < 0.05$) (Figure 2D). However, GM6001 had no inhibitory effect on MMP-2 activity in these cells, suggesting that the observed effects of GM6001 were mediated primarily through ADAM-17 inhibition. In order to further validate or refute that GM6001 mediates its effects via MMPs other than ADAM-17, we analyzed the effect of GM6001 on MMPs and their endogenous inhibitors (TIMPs) in RASFs, using an antibody-based human MMP array kit (catalog no. AAH-MMP-1; RayBiotech). The results showed that GM6001 modestly inhibited TNFα/IFNγ-induced MMP-1, MMP-3, and TIMP-2 expression in RASFs (Figure 2E).

To further validate the mediatory role of ADAM-17 in FKN shedding, we performed siRNA studies targeting ADAM-17 and ADAM-10. First, we confirmed that an siRNA concentration of 50 pmoles is required for complete inhibition of ADAM-17 or ADAM-10 (Figure 2F). The transfection of RASFs with ADAM-10 siRNA caused no decrease in TNFα/IFNγ-induced sFKN production as compared with the control siRNA values (Figure 2G). However, the knockdown of ADAM-17 using siRNA caused an almost 33% decrease in TNFα/IFNγ-induced sFKN production when compared with the control siRNA levels ($P < 0.05$) (Figure 2G). These results further proved that ADAM-17, but not ADAM-10, is partly involved in FKN shedding in RASFs.

Essential role of p38 MAPK, cathepsins, and proteasome pathways in mediating TNFα/IFNγ-induced sFKN production in RASFs. To study the signaling pathways involved in the synthesis and release of TNFα/IFNγ-induced FKN, we pretreated RASFs with inhibitors of PKC (Ro-31; 10 μM), proteasome activity (MG132; 10 μM), p38 MAPK (SB203580; 10 μM), JNK/SAPK (SP600125; 10 μM), ERK-1/2 (PD98059; 10 μM), and STAT-3 (AG-490; 10 μM) for 2 hours, followed by stimulation with TNFα/IFNγ for 72 hours. The results showed that pretreatment with MG132 completely blocked TNFα/IFNγ-induced sFKN production in RASFs ($P < 0.05$) (Figure 3A). We observed 44% inhibition in stimulated sFKN production by the p38 MAPK inhibitor ($P < 0.05$) (Figure 3A), suggesting that TNFα/IFNγ induced sFKN production by activating the proteasome and p38 MAPK pathways.

Because multiple proteasome enzymes are in-

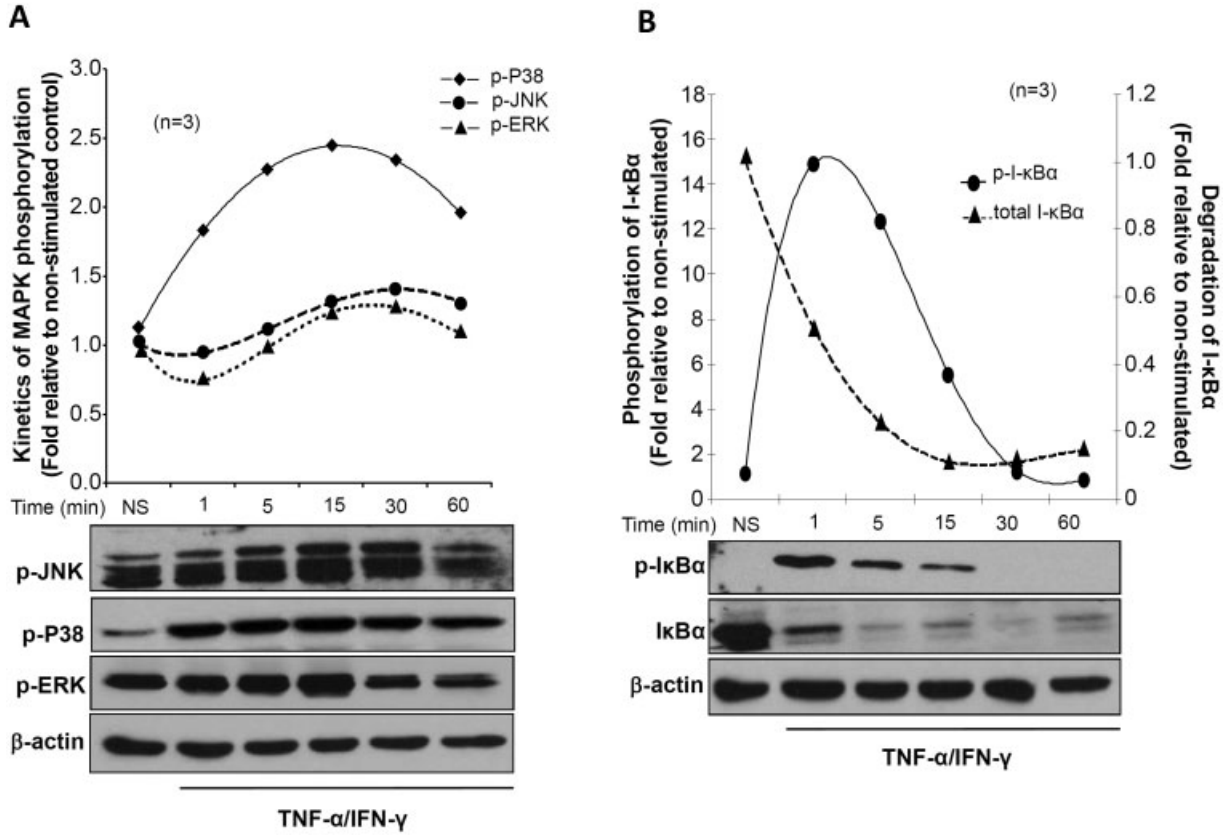

Figure 4. The combination of TNFα and IFNγ preferentially induces rapid phosphorylation of p38 MAPK and IκBα in RASFs, with subsequent degradation of IκBα. RASFs (2×10^5/well) were stimulated with TNFα/IFNγ for 1–60 minutes in serum-free RPMI 1640. Cells were lysed in extraction buffer containing protease inhibitors and used to determine phosphorylation of MAPKs (**A**) and the level of total and phosphorylated IκBα in RASFs (using Western blotting) (**B**). The intensity of the bands was quantified using ImageJ software. Values are the mean of cells from 3 independent donors treated under similar conditions. See Figure 1 for other definitions.

volved in the processing and shedding of cytokines and chemokines and their receptors, we investigated the role of 2 specific protease groups (cathepsin and calpain) in mediating this effect. RASFs were pretreated with inhibitors of calpain (calpeptin), cathepsin (cathepsin I), or proteasome activity (MG132) followed by stimulation with TNFα/IFNγ for 72 hours (27,28). The conditioned medium was analyzed for sFKN production. The results showed that blockade of cathepsin caused complete inhibition of sFKN release, as also observed with MG132 ($P < 0.05$) (Figure 3B). However, pretreatment with calpeptin resulted in no inhibition of TNFα/IFNγ-induced sFKN production, suggesting that cathepsins are the primary lysosomal proteins (besides protease enzymes) involved in proteolytic shedding of FKN in RASFs. TNFα/IFNγ-induced sFKN production was also observed following pretreatment with a protein synthesis inhibitor (cycloheximide) and an mRNA synthesis inhibitor (actinomycin D), further implying that inhibition of the proteasome pathway may block FKN expression in RASFs at any of these levels (Figure 3C).

Effect of TNFα/IFNγ in inducing activation of the p38 MAPK pathway in RASFs. To further extend this observation and test the effects of TNFα/IFNγ in inducing signaling pathways that mediate FKN expression and shedding, we treated RASFs with TNFα/IFNγ for 1–60 minutes and assessed the signaling mechanism. The results showed that TNFα/IFNγ induced phosphorylation of JNK/SAPK and ERK-1/2 after 30 minutes of stimulation (Figure 4A). Interestingly, a marked spontaneous increase in phosphorylated p38 MAPK levels was observed within 1 minute of TNFα/IFNγ stimulation, which persisted for up to 60 minutes ($P < 0.05$) (Figure 4A). The kinetics of MAPK phosphorylation, as determined by densitometric analysis, showed that TNFα/IFNγ stimulation resulted in a 2–3-fold increase in phosphorylated p38 MAPK levels when compared with untreated samples, and this activation continued

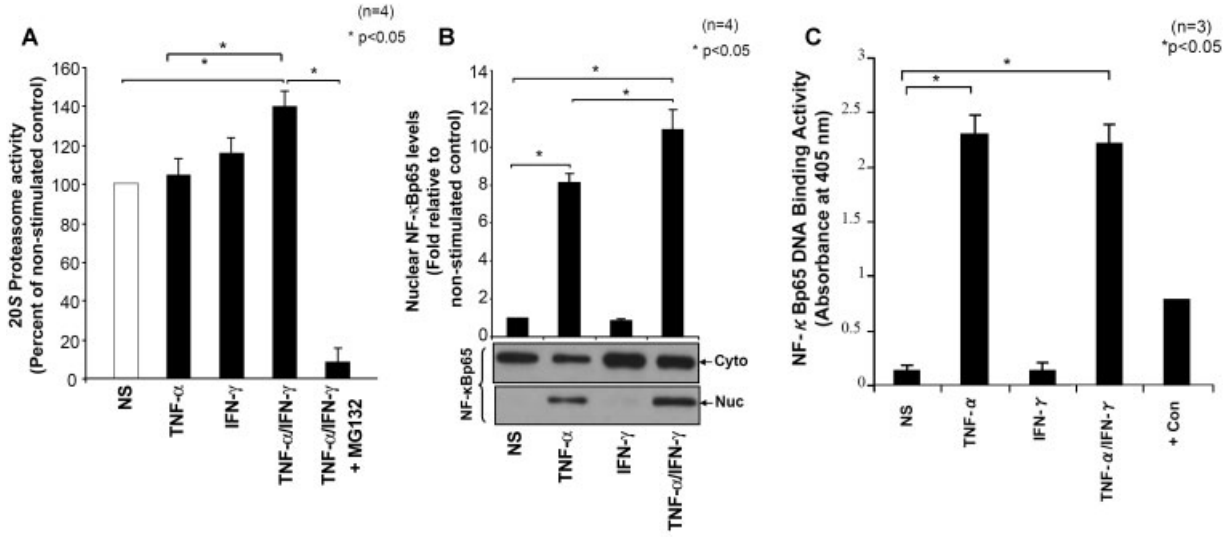

Figure 5. Coordinated effect of TNFα and IFNγ in inducing RASF 20S proteasomal activity. **A,** Activity of 20S proteasome in RASFs incubated with TNFα (20 ng/ml) and/or IFNγ (10 ng/ml) for 72 hours in serum-free RPMI 1640. **B,** NF-κB/p65 levels in the cytoplasmic (Cyto) and nuclear (Nuc) fractions of RASF lysates treated with TNFα, IFNγ, or TNFα/IFNγ, as determined by Western blotting. **C,** DNA binding of NF-κB/p65, as determined by enzyme-linked immunosorbent assay. Values are the mean ± SEM. Con = control (see Figure 1 for other definitions).

throughout the period of stimulation (Figure 4A). These results suggested that p38 MAPK was the primary signaling pathway used by TNFα/IFNγ to induce FKN expression in RASFs.

Further analysis showed that stimulation of RASFs with TNFα/IFNγ resulted in immediate phosphorylation of IκBα, which completely disappeared after 15 minutes of TNFα/IFNγ stimulation (Figure 4B). Interestingly, we observed the degradation of IκBα, starting within minutes of TNFα/IFNγ stimulation, with complete depletion occurring within 15 minutes (Figure 4B) ($P < 0.05$ versus not stimulated). These findings underline the importance of the proteasome pathway in mediating the activation and nuclear translocation of NF-κB/p65 via the proteasomal degradation of IκBα induced by TNFα/IFNγ stimulation.

Coordination of TNFα and IFNγ to induce 20S proteasome activity in RASFs. To validate the involvement of the proteasome pathway in the shedding and release of sFKN, we determined the 20S proteasomal activity in the treated samples, and also probed the lysates that had been treated for different time points, to study the effect of TNFα/IFNγ on NF-κB/p65 activation (Figure 5). The results of an ELISA showed that RASFs constitutively exhibited high 20S proteasomal activity (Figure 5A). Stimulation with TNFα or IFNγ for 24 hours resulted in modest increases (5% and 16%, respectively) in 20S proteasome activity compared with the untreated samples. However, we observed a significant 40% increase in 20S proteasome activity in RASFs in the presence of TNFα/IFNγ ($P < 0.05$) (Figure 5A). Pretreatment of RASFs with MG132 completely blocked TNFα/IFNγ-induced as well as constitutive proteasomal activity ($P < 0.05$) (Figure 5A).

Synergism of TNFα-induced activation of NF-κB/p65 in RASFs by IFNγ. To further correlate the impact of TNFα/IFNγ synergism, we determined NF-κB/p65 levels in the cytoplasmic and nuclear fractions of RASF lysates treated with TNFα, IFNγ, or TNFα/IFNγ for 30 minutes (Figure 5). IFNγ alone had no inducing effect on NF-κB/p65 nuclear translocation but modestly increased its cytoplasmic pool in the treated RASFs when compared with the untreated samples (Figure 5B). In addition, TNFα alone significantly induced the activation and nuclear translocation of NF-κB/p65, which was further increased (by ~25%) in the presence of IFNγ ($P < 0.05$) (Figure 5B). However, the results obtained from the NF-κB/p65 DNA-binding ELISA showed that the combination of TNFα and IFNγ did not induce synergy in the DNA-binding activity (Figure 5C), suggesting that increased nuclear translocation of NF-κB/p65 may be one of the potential mechanisms for the sustained activation and release of sFKN in RASFs.

Correlation of increased FKN expression and increased ADAM-17, ADAM-10, and phospho–p38 MAPK expression in the ankles of rats with AIA. Current understanding based on preclinical models of RA suggests the importance of proteasome activity in

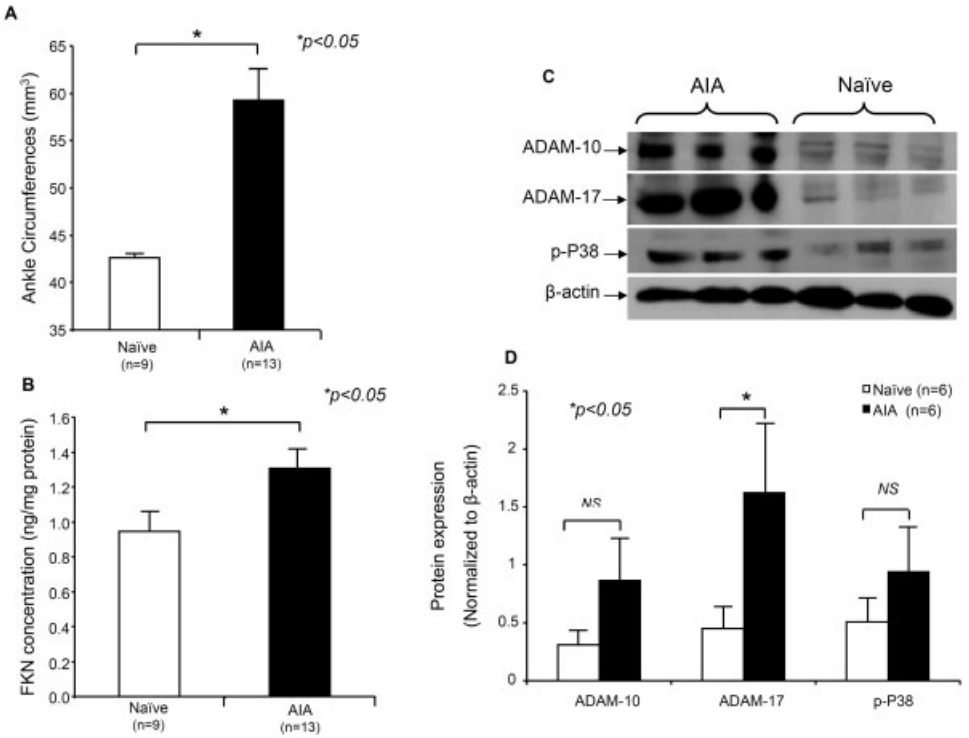

Figure 6. Increased expression of fractalkine (FKN) correlates with the expression of ADAM-10, ADAM-17, and phospho–p38 MAPK in rat adjuvant-induced arthritis (AIA). **A,** Ankle circumferences of naive rats and rats with AIA on day 17 following adjuvant injection. **B,** FKN levels in naive rats and rats with AIA, as determined by enzyme-linked immunosorbent assay. **C,** Expression of ADAM-10, ADAM-17, and phospho–p38 MAPK in joint homogenates from rats with AIA and naive rats, as determined by Western blotting. The intensity of the protein bands was quantified using ImageJ software. **D,** Protein expression of ADAM-10, ADAM-17, and phospho–p38 MAPK in the ankles of naive rats and rats with AIA, as determined by densitometry. Bars show the mean ± SEM. NS = not significant.

disease progression (29,30). However, there is a significant gap in the understanding of the role of ADAMs in the tissue destruction process in RA. To address the role of ADAMs and also correlate it with FKN expression, we determined FKN levels in joint homogenates, using a rat ELISA kit (R&D Systems), and evaluated the expression of ADAM-17, ADAM-10, and phospho–p38 MAPK by Western blotting.

Results of the analysis showed that severe arthritis developed in the rats 17 days after administration of adjuvant, as determined by ankle circumferences ($P < 0.05$) (Figure 6A). Analysis of FKN levels using a rat ELISA revealed that FKN was constitutively present in high quantities in naive rats, and this expression was further increased (by ~30%) in rats with AIA compared with rats in the naive group ($P < 0.05$) (Figure 6B). Western blot analysis of joint homogenates showed a marked increase in ADAM-10, ADAM-17, and phospho–p38 MAPK expression in rats with AIA compared with rats in the naive group (Figure 6C). Densitometric analysis of the protein expression showed approximately 2-fold, 4-fold, and 2-fold increases in the expression of ADAM-10, ADAM-17, and phospho–p38 MAPK, respectively, in the ankles of rats with AIA compared with rats in the naive group ($P < 0.05$) (Figure 6D). Interestingly, the increase in ADAM-17 expression was almost 2-fold higher than the increase in ADAM-10 expression, suggesting the critical involvement of ADAM-17 in RA pathogenesis in this model of human RA.

DISCUSSION

In recent years, FKN has emerged as one of the potential molecules that play an important pathologic role in chronic inflammatory diseases including cancer and RA (10,11). Despite a significant understanding of the role of FKN in propagating these diseases, there has been limited progress in developing pharmacologic interventions aimed at therapeutic suppression of FKN function and activity. This may be partly attributed to a limited understanding of the molecular mechanisms

that govern its synthesis and release in different cell types or tissues. In this regard, the present study provides evidence of the timely synthesis and shedding of FKN in response to TNFα/IFNγ stimulation, the signaling mechanisms that govern its expression in RASFs, and the role of identified signaling pathways (primarily p38 MAPK, cathepsin, and proteasome) in rat AIA that may potentially be involved in the regulation of FKN expression.

RASFs are actively involved in both cell adhesion and cell chemoattraction by producing adhesion molecules, such as intercellular adhesion molecule 1 or vascular cell adhesion molecule 1, and peppering out soluble chemokines, such as sFKN, to attract leukocytes and other inflammatory cells (10). Previous studies suggest that RASF FKN is synthesized and released as a soluble form long after stimulation with TNFα and IFNγ (16). In the present study, we observed that TNFα and IFNγ synergistically induced FKN expression as early as 6 hours followed by its release that continued up to 72 hours. To our knowledge, this is the first time that time-dependent expression and shedding of FKN in RASFs have been determined. Hence, evaluation of the signaling pathways and catalytic enzymes involved in FKN processing may serve as a targeted therapeutic approach to suppress the participation of FKN in chemotaxis. To further extend this observation in the rat model of AIA, we determined the levels of FKN in the joint homogenates of rats with AIA and naive rats. Although the constitutive levels of FKN were high in the joint homogenates of naive rats, FKN expression further increased by ~30% in the AIA group compared with the naive group, suggesting its increased expression during inflammation and tissue destruction in RA.

As FKN is expressed, it is transported to the cell membrane, where it becomes available for shedding and release as a soluble FKN in a controlled manner under the influence of proteolytic enzymes (14,31). ADAM-17, as well as other proteases such as ADAM-10, cleaves membrane-bound FKN, whereas the soluble form is released to chemoattract monocytes, natural killer cells, and T cells (12–14,32). However, the roles that ADAM-17, ADAM-10, or other proteases play in FKN processing has been shown to be cell or tissue specific. For example, ADAM-17 has been shown to centrally regulate the conversion of FKN from a membrane-bound adhesion molecule to a soluble chemoattractant in human umbilical vein endothelial cells (12). In contrast, the proinflammatory cytokine–induced sFKN in Hep-G2 cells observed in a recent study was suggested to be regulated independently of ADAM-17 activity (33). Results from another study using hepatic stellate cells suggested that both ADAM-10 and ADAM-17, in addition to MMP-2, mediate FKN shedding to recruit inflammatory cells and stimulate chronic hepatic inflammation in a paracrine manner (34). However, no such study has been reported in RASFs or osteoarthritis SFs.

Partial inhibition of FKN expression and release by ADAM-17 inhibition using siRNA and chemical inhibitor approaches provide evidence for the role of ADAM-17, at least in part, and other signaling pathways in mediating TNFα/IFNγ-induced FKN expression and shedding in RASFs. Furthermore, the lack of translation of ADAM-10 protein or the inability of a caspase 3 inhibitor to block FKN in response to TNFα/IFNγ suggests a limited role or no role of these enzymes in the processing of RASF FKN under inflammatory conditions.

To further understand the pathologic significance of these in vitro observations, we further validated these findings in a rat model of AIA. Previous studies have proven the efficacy of proteasome inhibitors in ameliorating rat AIA (29,30). Although several ADAM-17/TACE inhibitors have been successfully tested in models of preclinical arthritis (35,36), the expression pattern and role of ADAM-10 or ADAM-17 in mediating proteolytic shedding of chemokines such as FKN in human synovial fibroblasts or joint destruction in animal models of arthritis are not fully understood. Results from this study provide novel evidence of the relative expression of ADAM-10 and ADAM-17 in the ankles of rats with AIA and further correlate with in vitro findings of increased ADAM-17 expression compared with ADAM-10 expression in RASFs. However, further studies are warranted to validate the selectivity of these ADAMs in regulating FKN expression in AIA and/or other models of RA using selective inhibitors of ADAM-10 or ADAM-17.

The MAPK family has always been an integral part of the signaling mechanism through which proinflammatory cytokines mediate their detrimental effects in RA and other rheumatic diseases (37). However, overlap or distinction of the role played by an individual kinase within the MAPK proteins varies depending on the stimulus, protein synthesized, and pathologic implications. For example, FKN was previously shown to stimulate ERK-1/2 and JNK pathways, and inhibition of the ERK-1/2 pathway results in decreased FKN-induced RASF migration (38). Similar studies showed that TNFα/IFNγ induced sFKN production after 72 hours of stimulation (16,38).

Despite the observation that the combination of TNFα and IFNγ causes synergistic induction of sFKN synthesis, not much is known in relation to the mechanism involved in the coordination of these 2 potent immunomodulatory molecules in the processing and shedding of FKN in RASFs. The results from the present study address that gap and suggest the potential role of p38 MAPK and proteasome pathways in sFKN production. The complete blockade of FKN expression and shedding by the proteasome or cathepsin inhibitor and the partial regulation by ADAM-17 inhibition suggest that these pathways play a crucial role in FKN synthesis and processing and may be exploited as therapeutic targets to suppress FKN expression and activity in RA. Furthermore, ~3-fold selective activation of p38 MAPK and the spontaneous phosphorylation and subsequent degradation of IκBα further authenticate the distinct roles these molecules play in mediating TNFα/IFNγ-induced FKN expression and shedding in RASFs. Parallel to these in vitro results, we observed increased expression of phosphorylated p38 MAPK in the ankles of rats with AIA compared with the naive group. These studies suggest that p38 MAPK may be closely involved in mediating joint inflammation in RA, at least in part, by up-regulating FKN synthesis and shedding.

ADAM-17, α-secretase, and γ-secretase have been shown to play an important role in the sequential proteolytic processing of transmembrane chemokines, including FKN and CXCL16 (39). However, our results suggest the importance of the pathologic role of ADAM-17 (along with that of traditionally known proteases) in mediating TNFα/IFNγ-induced FKN expression and shedding in RASFs and in rat AIA. In addition, we were able to show that among different protease groups, lysosomal cathepsins also play an important role in the proteolytic shedding of sFKN. Notably, this study is the first to demonstrate the proportionally higher expression of ADAM-17 compared with ADAM-10 in the ankles of rats with AIA and provides an opportunity to test whether modulation of ADAM-17 or ADAM-10 may ameliorate arthritis in this model of human RA. In addition, the current findings also validate the contribution of p38 MAPK and proteasome pathways in further amplifying this process. These findings may potentially be extended to evaluate the role of these mediators in the processing and maturation of other potential chemokines and cytokines, such as CXCL16, in RA pathogenesis. However, further studies are warranted to better understand the positive or negative influence of other proinflammatory cytokines such as IL-1β or IL-6, alone or in combination with IFNγ, on FKN synthesis and shedding in RASFs or rat AIA.

In conclusion, the results of the current study suggest that the combination of TNFα and IFNγ plays an important role and acts in a time-dependent manner to rapidly induce FKN expression and release. In this study, we closely evaluated the early events, with a concomitant focus on the cell-signaling mechanisms governing FKN synthesis and shedding. Our results suggest that FKN may be therapeutically targeted at various steps of its processing to limit its role as an adhesion molecule or a soluble chemoattractant in RA and possibly other systemic inflammatory diseases.

ACKNOWLEDGMENTS

We thank Dr. Nabil Ebraheim (Department of Orthopaedic Surgery, University of Toledo), the National Disease Research Interchange, and the Cooperative Human Tissue Network for providing RA synovial tissue. We also thank Dr. David Fox (University of Michigan, Ann Arbor) for providing some of the RASFs.

AUTHOR CONTRIBUTIONS

All authors were involved in drafting the article or revising it critically for important intellectual content, and all authors approved the final version to be published. Dr. Ahmed had full access to all of the data in the study and takes responsibility for the integrity of the data and the accuracy of the data analysis.

Study conception and design. Jones, Ahmed.

Acquisition of data. Jones, Riegsecker, Rahman, Beamer, Aboualaiwi, Ahmed.

Analysis and interpretation of data. Jones, Riegsecker, Rahman, Khuder, Ahmed.

REFERENCES

1. Pope RM. Apoptosis as a therapeutic tool in rheumatoid arthritis. Nat Rev Immunol 2002;2:527–35.
2. Iwamoto T, Okamoto H, Toyama Y, Momohara S. Molecular aspects of rheumatoid arthritis: chemokines in the joints of patients. FEBS J 2008;275:4448–55.
3. Patel DD, Zachariah JP, Whichard LP. CXCR3 and CCR5 ligands in rheumatoid arthritis synovium. Clin Immunol 2001;98:39–45.
4. Katschke KJ Jr, Rottman JB, Ruth JH, Qin S, Wu L, LaRosa G, et al. Differential expression of chemokine receptors on peripheral blood, synovial fluid, and synovial tissue monocytes/macrophages in rheumatoid arthritis. Arthritis Rheum 2001;44:1022–32.
5. Zlotnik A, Yoshie O. Chemokines: a new classification system and their role in immunity. Immunity 2000;12:121–7.
6. Stievano L, Piovan E, Amadori A. C and CX3C chemokines: cell sources and physiopathological implications. Crit Rev Immunol 2004;24:205–28.
7. Ikejima H, Imanishi T, Tsujioka H, Kashiwagi M, Kuroi A, Tanimoto T, et al. Upregulation of fractalkine and its receptor, CX3CR1, is associated with coronary plaque rupture in patients with unstable angina pectoris. Circ J 2010;74:337–45.
8. Moatti D, Faure S, Fumeron F, Amara M, Seknadji P, McDermott DH, et al. Polymorphism in the fractalkine receptor CX3CR1 as a

genetic risk factor for coronary artery disease. Blood 2001;97: 1925–8.
9. Marchesi F, Locatelli M, Solinas G, Erreni M, Allavena P, Mantovani A. Role of CX3CR1/CX3CL1 axis in primary and secondary involvement of the nervous system by cancer. J Neuroimmunol 2010;224:39–44.
10. Jones BA, Beamer M, Ahmed S. Fractalkine/CX3CL1: a potential new target for inflammatory diseases. Mol Interv 2010;10:263–70.
11. Jones B, Koch AE, Ahmed S. Pathological role of fractalkine/CX3CL1 in rheumatic diseases: a unique chemokine with multiple functions. Front Immunol 2011;2:82.
12. Garton KJ, Gough PJ, Blobel CP, Murphy G, Greaves DR, Dempsey PJ, et al. Tumor necrosis factor-α-converting enzyme (ADAM-17) mediates the cleavage and shedding of fractalkine (CX3CL1). J Biol Chem 2001;276:37993–8001.
13. Hundhausen C, Misztela D, Berkhout TA, Broadway N, Saftig P, Reiss K, et al. The disintegrin-like metalloproteinase ADAM-10 is involved in constitutive cleavage of CX3CL1 (fractalkine) and regulates CX3CL1-mediated cell-cell adhesion. Blood 2003;102: 1186–95.
14. Hundhausen C, Schulte A, Schulz B, Andrzejewski MG, Schwarz N, von Hundelshausen P, et al. Regulated shedding of transmembrane chemokines by the disintegrin and metalloproteinase 10 facilitates detachment of adherent leukocytes. J Immunol 2007; 178:8064–72.
15. Ruth JH, Volin MV, Haines GK III, Woodruff DC, Katschke KJ Jr, Woods JM, et al. Fractalkine, a novel chemokine in rheumatoid arthritis and in rat adjuvant-induced arthritis. Arthritis Rheum 2001;44:1568–81.
16. Volin MV, Huynh N, Klosowska K, Chong KK, Woods JM. Fractalkine is a novel chemoattractant for rheumatoid arthritis fibroblast-like synoviocyte signaling through MAP kinases and Akt. Arthritis Rheum 2007;56:2512–22.
17. Moon SO, Kim W, Sung MJ, Lee S, Kang KP, Kim DH, et al. Resveratrol suppresses tumor necrosis factor-α-induced fractalkine expression in endothelial cells. Mol Pharmacol 2006;70: 112–9.
18. Garcia GE, Xia Y, Chen S, Wang Y, Ye RD, Harrison JK, et al. NF-κB-dependent fractalkine induction in rat aortic endothelial cells stimulated by IL-1β, TNFα, and LPS. J Leukoc Biol 2000;67: 577–84.
19. Matsumiya T, Ota K, Imaizumi T, Yoshida H, Kimura H, Satoh K. Characterization of synergistic induction of CX3CL1/fractalkine by TNFα and IFN-γ in vascular endothelial cells: an essential role for TNFα in post-transcriptional regulation of CX3CL1. J Immunol 2010;184:4205–14.
20. D'Haese JG, Demir IE, Friess H, Ceyhan GO. Fractalkine/CX3CR1: why a single chemokine-receptor duo bears a major and unique therapeutic potential. Expert Opin Ther Targets 2010;14: 207–19.
21. Wiener JJ, Sun S, Thurmond RL. Recent advances in the design of cathepsin S inhibitors. Curr Top Med Chem 2010;10:717–32.
22. Arnett FC, Edworthy SM, Bloch DA, McShane DJ, Fries JF, Cooper NS, et al. The American Rheumatism Association 1987 revised criteria for the classification of rheumatoid arthritis. Arthritis Rheum 1988;31:315–24.
23. Ahmed S, Marotte H, Kwan K, Ruth JH, Campbell PL, Rabquer BJ, et al. Epigallocatechin-3-gallate inhibits IL-6 synthesis and suppresses transsignaling by enhancing soluble gp130 production. Proc Natl Acad Sci U S A 2008;105:14692–7.
24. Ahmed S, Pakozdi A, Koch AE. Regulation of interleukin-1β–induced chemokine production and matrix metalloproteinase 2 activation by epigallocatechin-3-gallate in rheumatoid arthritis synovial fibroblasts. Arthritis Rheum 2006;54:2393–401.
25. Ahmed S, Silverman MD, Marotte H, Kwan K, Matuszczak N, Koch AE. Down-regulation of myeloid cell leukemia 1 by epigallocatechin-3-gallate sensitizes rheumatoid arthritis synovial fibroblasts to tumor necrosis factor α–induced apoptosis. Arthritis Rheum 2009;60:1282–93.
26. Marotte H, Ruth JH, Campbell PL, Koch AE, Ahmed S. Green tea extract inhibits chemokine production, but up-regulates chemokine receptor expression, in rheumatoid arthritis synovial fibroblasts and rat adjuvant-induced arthritis. Rheumatology (Oxford) 2010;49:467–79.
27. Zhu DM, Uckun FM. Cathepsin inhibition induces apoptotic death in human leukemia and lymphoma cells. Leuk Lymphoma 2000;39:343–54.
28. Morita M, Banno Y, Dohjima T, Nozawa S, Fushimi K, Fan DG, et al. μ-Calpain is involved in the regulation of TNFα-induced matrix metalloproteinase-3 release in a rheumatoid synovial cell line. Biochem Biophys Res Commun 2006;343:937–42.
29. Ahmed AS, Li J, Ahmed M, Hua L, Yakovleva T, Ossipov MH, et al. Attenuation of pain and inflammation in adjuvant-induced arthritis by the proteasome inhibitor MG132. Arthritis Rheum 2010;62:2160–9.
30. Yannaki E, Papadopoulou A, Athanasiou E, Kaloyannidis P, Paraskeva A, Bougiouklis D, et al. The proteasome inhibitor bortezomib drastically affects inflammation and bone disease in adjuvant-induced arthritis in rats. Arthritis Rheum 2010;62: 3277–88.
31. Ludwig A, Weber C. Transmembrane chemokines: versatile 'special agents' in vascular inflammation. Thromb Haemost 2007;97: 694–703.
32. Bazan JF, Bacon KB, Hardiman G, Wang W, Soo K, Rossi D, et al. A new class of membrane-bound chemokine with a CX3C motif. Nature 1997;385:640–4.
33. Turner SL, Mangnall D, Bird NC, Blair-Zajdel ME, Bunning RA. Effects of pro-inflammatory cytokines on the production of soluble fractalkine and ADAM17 by HepG2 cells. J Gastrointestin Liver Dis 2010;19:265–71.
34. Bourd-Boittin K, Basset L, Bonnier D, L'Helgoualc'h A, Samson M, Theret N. CX3CL1/fractalkine shedding by human hepatic stellate cells: contribution to chronic inflammation in the liver. J Cell Mol Med 2009;13:1526–35.
35. Qian M, Bai SA, Brogdon B, Wu JT, Liu RQ, Covington MB, et al. Pharmacokinetics and pharmacodynamics of DPC 333 ((2R)-2-((3R)-3-amino-3{4-[2-methyl-4-quinolinyl) methoxy] phenyl}-2-oxopyrrolidinyl)-N-hydroxy-4-methylpentanamide)), a potent and selective inhibitor of tumor necrosis factor α-converting enzyme in rodents, dogs, chimpanzees, and humans. Drug Metab Dispos 2007;35:1916–25.
36. Beck G, Bottomley G, Bradshaw D, Brewster M, Broadhurst M, Devos R, et al. (E)-2(R)-[1(S)-(Hydroxycarbamoyl)-4-phenyl-3-butenyl]-2′-isobutyl-2′-(methanesulfonyl)-4-methylvalerohydrazide (Ro 32-7315), a selective and orally active inhibitor of tumor necrosis factor-α convertase. J Pharmacol Exp Ther 2002;302: 390–6.
37. Ralph JA, Morand EF. MAPK phosphatases as novel targets for rheumatoid arthritis. Expert Opin Ther Targets 2008;12: 795–808.
38. Volin MV, Huynh N, Klosowska K, Reyes RD, Woods JM. Fractalkine-induced endothelial cell migration requires MAP kinase signaling. Pathobiology 2010;77:7–16.
39. Schulte A, Schulz B, Andrzejewski MG, Hundhausen C, Mletzko S, Achilles J, et al. Sequential processing of the transmembrane chemokines CX3CL1 and CXCL16 by α- and γ-secretases. Biochem Biophys Res Commun 2007;358:233–40.